Journal Pre-proof

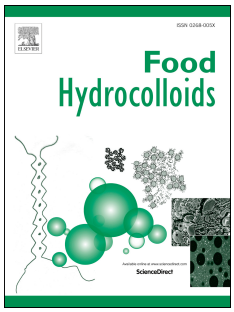

Hydroxypropyl methylcellulose and hydroxypropyl starch: Rheological and gelation effects on the phase structure of their mixed hydrocolloid system

Yanfei Wang, Long Yu, Qingjie Sun, Fengwei Xie

PII: S0268-005X(21)00014-X

DOI: https://doi.org/10.1016/j.foodhyd.2021.106598

Reference: FOOHYD 106598

To appear in: *Food Hydrocolloids*

Received Date: 24 November 2020

Revised Date: 25 December 2020

Accepted Date: 6 January 2021

Please cite this article as: Wang, Y., Yu, L., Sun, Q., Xie, F., Hydroxypropyl methylcellulose and hydroxypropyl starch: Rheological and gelation effects on the phase structure of their mixed hydrocolloid system, *Food Hydrocolloids*, https://doi.org/10.1016/j.foodhyd.2021.106598.

CRediT author statement:

Yanfei Wang: Conceptualization, Methodology, Validation, Formal Analysis, Investigation, Data Curation, Visualisation, Funding acquisition. **Long Yu:** Conceptualization, Methodology, Resources, Supervision, Project administration, Funding acquisition. **Qingjie Sun:** Funding acquisition. **Fengwei Xie:** Conceptualization, Methodology, Visualisation, Writing - Review & Editing.

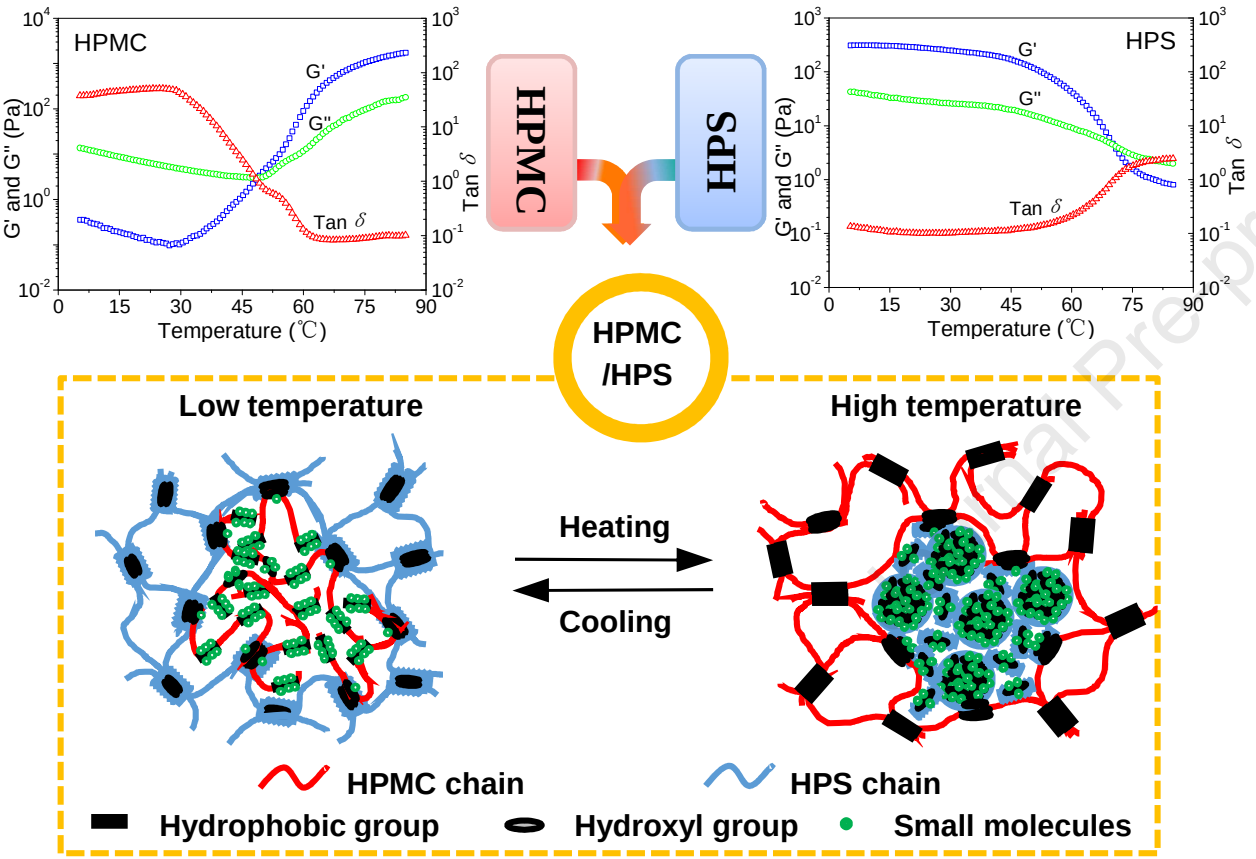

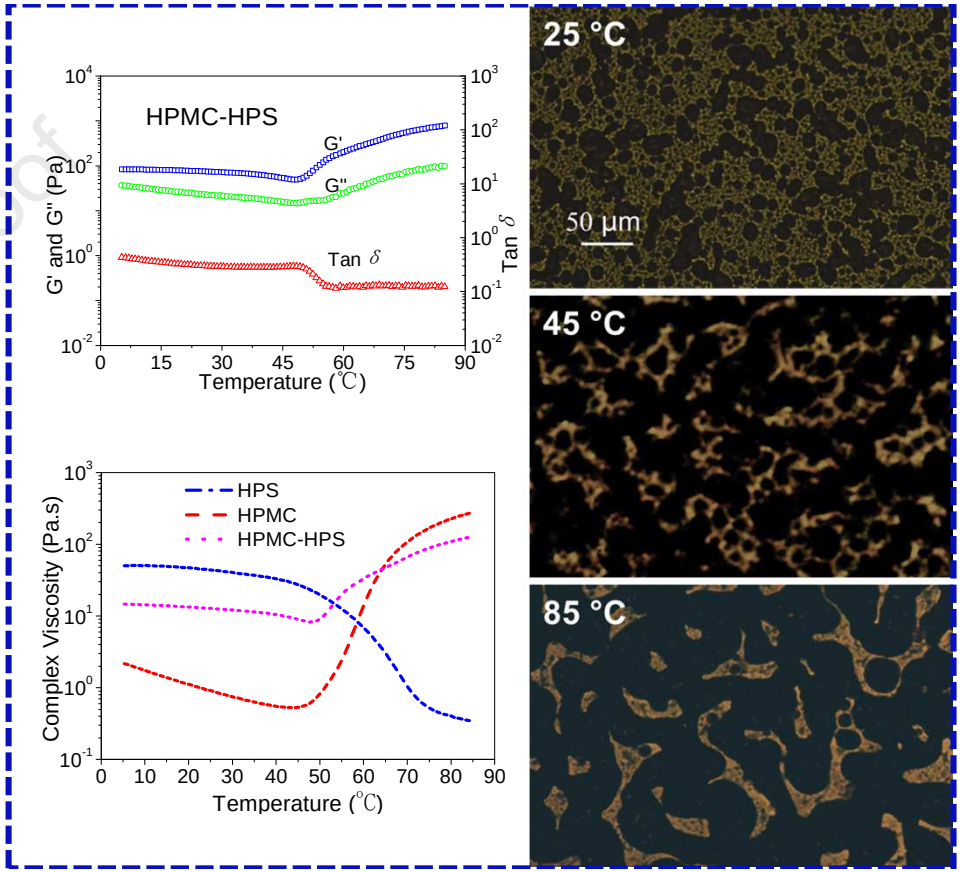

Hydroxypropyl methylcellulose and hydroxypropyl starch: Rheological and gelation effects on the phase structure of their mixed hydrocolloid system

Yanfei Wang[1,2,3], Long Yu[3,*], Qingjie Sun[1,2], Fengwei Xie[4,†]

[1]*College of Food Science and Engineering, Qingdao Agricultural University, Qingdao, Shandong 266109, China*

[2]*Qingdao Special Food Research Institute, Qingdao, Shandong 266109, China*

[3]*College of Food Science and Engineering, South China University of Technology, Guangzhou, Guangdong 510640, China*

[4]*International Institute for Nanocomposites Manufacturing (IINM), WMG, University of Warwick, Coventry CV4 7AL, United Kingdom*

[*]Corresponding author. *E-mail address*: felyu@scut.edu.cn (L. Yu),

[†]Corresponding author. *E-mail addresses*: d.xie.2@warwick.ac.uk; fwhsieh@gmail.com (F. Xie)

Abstract

It is common to hybridize biopolymers for developing materials with combined properties or functionality. However, biopolymers are usually not fully compatible despite their chemical similarity, posing challenges to create mixed systems. Herein, we investigated how the gelation behavior and rheological properties of hydroxypropyl methylcellulose (HPMC), a thermal gel, and hydroxypropyl starch (HPS), a cooling gel, affect their miscibility and the phase structure of their mixed system. The dependence of the zero-shear viscosity for HPMC/HPS paste on biopolymer concentration in a double-logarithmic coordinate can be divided into two parts with the slopes being 11.9 and 2.8 respectively, indicating different degrees of intermolecular entanglement. A typical "sea-island" morphology was shown in the blends, and the phase structure (continuous or discrete) changed with varying HPMC/HPS blend ratio and temperature. This phase structure change can be well correlated to rheological parameters such as zero-shear viscosity, loss tangent, complex viscosity, and the Arrhenius equation correction coefficient (α). Biopolymer concentration, HPMC/HPS ratio, and temperature together controlled rheological properties and phase distribution for the mixed system. The relationship between rheological behavior and phase structure for HPMC/HPS understood from this work provides an insight into designing mixed biopolymer systems with desirable processability, structure, and properties.

Keywords: Hydroxypropyl methylcellulose; Hydroxypropyl starch; Rheological properties; Biopolymer phase structure; Biopolymer blends

1 Introduction

As a modified biopolymer, hydroxypropyl methylcellulose (HPMC) has been widely applied in different applications such as edible packaging, medicinal capsules, and drug delivery systems due to its water-solubility and biodegradability and excellent film-forming, mechanical and barrier properties (Al-Tabakha, 2010; Muhammad-Javeed & Mohammed, 2018; Siepmann & Peppas, 2012). However, the low oxygen-barrier property (Ghadermazi, Hamdipour, Sadeghi, Ghadermazi, & Asl, 2019; Hay, et al., 2018; Y. F. Wang, Yu, et al., 2016), high production energy consumption (Zhang, et al., 2013), and high price of HPMC (Allenspach, Timmins, Sharif, & Minko, 2020) pose strong limits for its applications. To cope with the property limitations of individual polymers, achieve enhanced and/or new material properties, reduce costs, and to expand applications, mixing different polymers is one of the most cost-effective methods (Aghjeh, Khonakdar, & Jafari, 2015; Botaro, de Freitas, do Carmo, & Raimundo, 2020; Jéssica Bassi da Silva, Michael Thomas Cook, & Bruschi, 2020; Xu, Wang, & Shi, 2020). Hydroxypropyl starch (HPS), a typical chemically modified starch with some original hydroxyl groups replaced with hydroxypropyl groups, is cheaper than HPMC, show excellent gas barrier property, and has been widely used in the food industry, therefore being an ideal substitute for part of HPMC (X. Chen, et al., 2019; J. Liu, Lai, Wang, Wang, & Liu, 2020; Qin, et al., 2019; W. W. Wang, Sun, & Shi, 2019).

The production of edible materials such as pre-formed films (medicinal capsules) or edible coating generally relies on wet processes that are based on film-forming solutions or dispersions (Cuq, Gontard, & Guilbert, 1998; Suhag, Kumar, Petkoska, & Upadhyay, 2020). Specifically, polymers are first dissolved or dispersed in a liquid and then dried. The design of such processes

(typically comprising pumping, casting, dipping, brushing, spraying, and drying) requires accurate data on the rheological properties of film-forming solutions or dispersions (Q. Wang, Yang, Chen, & Shao, 2012). In turn, rheological properties also play an important role in controlling the quality of coating films (Peressini, Bravin, Lapasin, Rizzotti, & Sensidoni, 2003; Xiao, Tong, & Lim, 2012).

For thermodynamic reasons, most polymer blends are immiscible on a molecular scale. Nevertheless, immiscible blends often turn out to be useful. For example, while polypropylene and polystyrene are immiscible, a polypropylene 90/polystyrene 10 blend, which showed a phase separation structure where polystyrene droplets were scattered in the polypropylene matrix, showed the maximum impact strength that blends at other ratios (R. Y. Chen, Liu, Han, Zhang, & Li, 2020). The degree of polymer miscibility largely influences the rheological properties of the mixed systems (Tanaka, Sako, Hiraoka, Yamaguchi, & Yamaguchi, 2020; Wongphan & Harnkarnsujarit, 2020). And, the rheological properties of polymer blends determine material phase structure (Ilyin, Makarova, Polyakova, & Kulichikhin, 2020; Xiao, Tong, Zhou, & Deng, 2015).

Considering that both HPMC and HPS are water-soluble polysaccharides and consist of the same original repeat unit (glucose with hydroxyl groups), there should be good compatibility between them. However, HPMC and HPS are hydrogels with opposite temperature-induced gelation behavior. Specifically, HPMC dissolves in water at a low temperature and congeals at a high temperature, whereas HPS undergoes gelation on cooling but solates upon heating (Polamaplly, et al., 2019; Qin, et al., 2019; Zhong, et al., 2020). The difference in gelation behavior between HPMC and HPS makes it challenging to achieve a blend of these two biopolymers with high miscibility and fine phase distribution. Moreover, the phase structure of HPMC and HPS should influence the mixed gel

properties. The rheological properties of HPMC/HPS blends depend on several factors such as biopolymer concentration, mixing ratio, temperature, and shear stress applied (Y. F. Wang, Zhang, et al., 2016). The manipulation of these factors can be used to further explore the relationship between microstructure and properties for thermal-/cooling-gel mixed systems.

In this work, the effects of solution concentration, mixing ratio, and temperature on the rheological properties and morphology of HPMC/HPS blends were investigated. A schematic model is proposed to describe temperature-induced phase structure changes for HPMC/HPS blends. The knowledge obtained from this work could also help in understanding the relationship between microstructure and processability for mixed systems based on biopolymers with different gelation behavior. The results could also be insightful for the design of similar biopolymer composite materials with tailored structure and properties.

2 Materials and method

2.1 Materials

A commercially available pharmaceutical-grade HPMC (HT-E15; viscosity at 2% concentration: 6.3 mPas; pH 6.0; methoxyl content on dry basis: 29%; hydroxypropyl oxygen content on dry basis 8.4%) was purchased from Huzhou Hopetop Pharmaceutical Co., Ltd (China). A food-grade maize HPS with a degree of substitution (DS) of 0.11 was supplied by Penford (Australia).

2.2 Sample preparation

HPMC/HPS solutions with different total biopolymer concentration (5–20 wt%) and weight ratio (0:10 to 10:0, w/w) were prepared. Specifically, HPMC and HPS in the form of dry powder were

firstly mixed and then dispersed in hot water (70 °C) with stirring for 30 min to ensure their proper dispersion. Then, using a water bath, the solutions were heated to 95 °C and maintained for 1 h with stirring to gelatinize HPS. Afterwards, the solutions were cooled to room temperature to dissolve HPMC under stirring before testing.

2.3 Rheological measurement

The rheological properties of HPMC/HPS pastes were investigated using a Discovery HR-2 rheometer (TA Instruments, New Castle, DE, USA). A parallel-plate geometry (40 mm diameter) with a gap of 0.5 mm was used for measurement.

To study the stability of HPMC/HPS pastes under shear, the samples were subjected to steady shear at a constant high shear rate of 800 s^{-1} for 2500 s at 25 °C and the change in viscosity was recorded.

Under steady shear, the viscosity of a polymer may change with time before a stable value is achieved (Tajuddin, Xie, Nicholson, Liu, & Halley, 2011). As a result, pre-shearing with a shear rate of 800 s^{-1} at room temperature (25 °C) for 1000 s was performed to ensure all samples to achieve a stable rheological state before immediate measurement. Shear viscosity was measured as a function of shear rate in the range of 10^{-2}–10^{3} s.

Three-interval thixotropy testing was performed to investigate the stability of HPMC/HPS pastes. This test was carried out at 25 °C at a low-shear stage with the shear rate kept at 1 s^{-1} for 50 s, then a high-shear stage with the shear rate kept at 1000 s^{-1} for 20 s, and finally, a structural recovery stage with the shear rate kept at 1 s^{-1} for 250 s.

Temperature sweeps were carried out from 5 °C to 85 °C with a heating rate of 2 °C/min under dynamic mode. The frequency was set at 1 Hz and the strain at 0.1% (to be in the linear range of viscoelasticity). The sample was placed between the parallel plates, and then a small amount of silicone oil was applied to the periphery of the sample to prevent moisture evaporation.

2.4 Microscopy observation and method of dying HPS

An Olympus BHZ-UMA optical microscope was used to image the morphology of HPMC/HPS pastes. The HPMC/HPS (5:5, w/w) solution of a concentration of 3 wt% was prepared using the same method mentioned above. The glass and the solution were kept at the same testing temperature and then the films were prepared by casting the solutions on glass at different temperatures (25 °C, 45 °C, and 85 °C). HPS was dyed with 1% iodine alcohol solution (prepared by mixing 1g of iodine and 10 g of potassium iodine solution in a 100 mL flask, with alcohol subsequently added) and dried at the same testing temperature.

3 Results and discussions

3.1 Time-dependence of HPMC/HPS paste viscosity

Fig. 1 shows the viscosity *vs.* time curves for HPMC/HPS blends with different selected blending ratio and concentrations at a constant shear rate of 800 s^{-1} (not all results presented here, as the trend was quite similar). For all blends, the viscosity decreased with time until a stable value was achieved. The time needed for achieving a stable state varied with HPMC/HPS ratio and total biopolymer concentration. After 1000 s, all the samples reached constant viscosity. Therefore, pre-shearing at 800 s^{-1} for 1000 s was performed for rheological tests for all the samples.

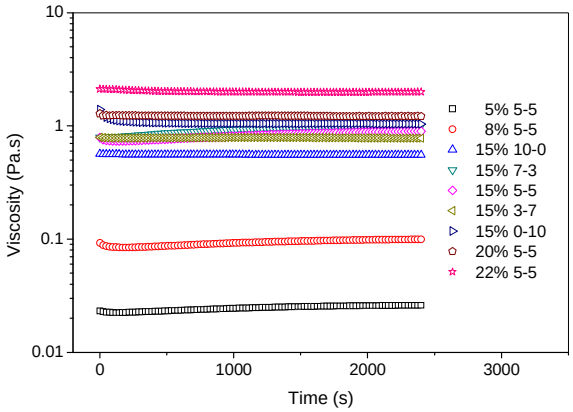

Fig. 1 Viscosity as a function of time for HPMC/HPS pastes. The shear rate was fixed at 800 s^{-1}.

3.2 Effect of biopolymer concentration on HPMC/HPS paste viscosity

Fig. 2(A) shows the viscosity *vs.* shear rate curves for HPMC/HPS pastes of different concentration. At a certain shear rate, increasing biopolymer concentration resulted in higher viscosity, which is as expected. For all HPMC/HPS pastes, the viscosity decreased with increasing shear rate, suggesting shear-thinning behavior. Moreover, the dependence of viscosity on shear rate depended on total biopolymer concentration. The shear-thinning behavior was more evident with a higher biopolymer concentration.

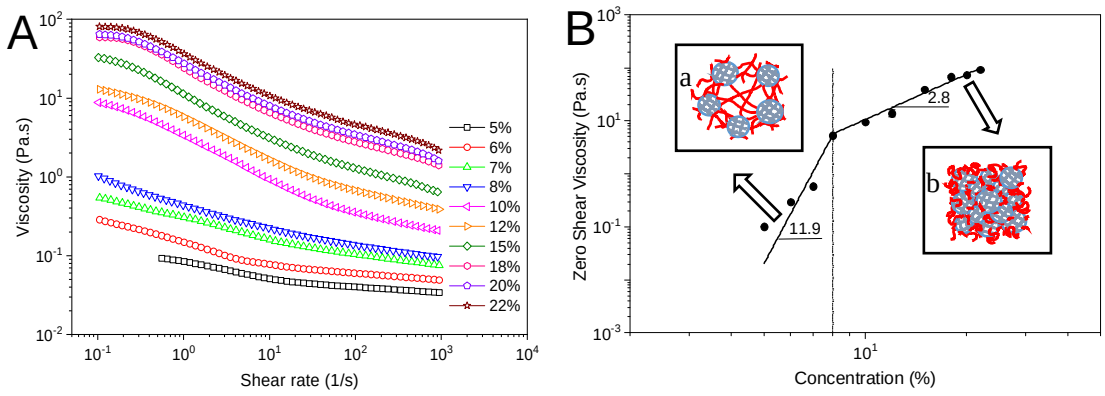

Fig. 2 A) Flow curves for 50:50 (w/w) HPMC/HPS pastes of different total biopolymer concentration at 25 °C; B) Zero-shear viscosity as a function of total biopolymer concentration, with the molecular conformation of HPMC/HPS schematically shown (the HPMC/HPS ratio was 50:50 (w/w), red lines represent HPMC chains and grey lines HPS).

The viscosity *vs.* shear rate curves for HPMC/HPS pastes were fitted with the Carreau model (Carreau, Pierre, & J., 1972) and then extrapolated to obtain zero-shear viscosity, η_0 ($0.9969 < R^2 < 0.9997$). **Fig. 2(B)** shows zero-shear viscosity as a function of total biopolymer concentration. It is noticeable that η_0 had a power-law dependence on biopolymer concentration as represented by the equation below:

$$\eta_0 = kC^m \qquad (1)$$

Where η_0 is the zero-shear viscosity, C is the total biopolymer concentration, k and m are constants.

The dependence of η_0 on biopolymer concentration in a double-logarithmic coordinate can be divided into two parts with the slopes (m) being 11.9 and 2.8, respectively. The critical concentration (C^*) that divides the two regions was about 8 wt%. According to the general relationship between biopolymer concentration dependence and the polymer state in solution (Colby, 2010), the likely molecular conformation of HPMC/HPS blends was proposed schematically in the inset of **Fig. 2(B)**.

As the lowest concentration (5 wt%) in our work is still much higher than those used in previous studies (0.05–1.3 wt%) (Morris, Cutler, Ross-Murphy, Rees, & Price, 1981; Pakravan, Heuzey, & Ajji, 2011; Tan, Li, Chen, & Xie, 2016), likely, the samples in both regions were in a concentrated state. In the first region ($C < C^*$), gelatinized HPS thickened at a low temperature and forms microgel, which interacts with HPMC chains at the microgel particle edge. HPS microgel particles

and HPMC chains tended to interact or entangle with each other due to the space-block effect and hydrogen bonding (inset a of **Fig. 2B**). The η_0 of HPMC/HPS paste increased rapidly with increasing concentration. In the second region ($C > C^*$), the interactions and entanglements were already denes enough (inset b of **Fig. 2B**) and their enhancement by increasing concentration was not as effective as in the first region. Thus, the slope for the second region was not as high as the first region.

For a polymer solution, the relationship between shear stress (τ) and shear rate (γ) can be described by the Ostwald-de Waele equation:

$$\tau = K\gamma^n \qquad (2)$$

Where K is the fluid consistency index and n is the flow behavior index. The values of K and n calculated for HPMC/HPS pastes of different concentration are shown in **Table 1**.

For a Newtonian fluid, n equals 1. Pseudoplastic fluids have $n < 1$, and greater deviation of n from 1 indicates stronger pseudoplastic (shear-thinning) behavior. **Table 1** shows that for all the samples, n is less than 1, indicating they were all pseudoplastic (shear-thinning). For HPMC/HPS pastes of low concentration (e.g. 5 wt%), the n values are close to 1, meaning they were more like a Newtonian fluid as HPMC chains and HPS microgel particles are mostly separated in the solution. Increasing concentration led to lower n, suggesting stronger shear-thinning behavior. The flow behavior of high-concentration samples is attributed to the interaction and entanglement among HPMC/HPS chains.

Table 1 Flow behavior index (n) and fluid consistency index (K) for 50:50 (w/w) HPS/HPMC pastes of different concentration at 25 °C.

Concentration (%)	n	K (Pa·s^n)	R^2

5	0.922±0.004 [a]	0.06±0.00	1.0000
6	0.909±0.001	0.09±0.00	1.0000
7	0.859±0.002	0.20±0.01	1.0000
8	0.842±0.001	0.28±0.01	0.9999
10	0.747±0.003	1.15±0.05	0.9981
12	0.735±0.005	2.34±0.07	0.9988
15	0.681±0.006	6.27±0.94	0.9993
18	0.678±0.006	13.37±0.88	0.9991
20	0.656±0.000	18.06±0.54	0.9984
22	0.653±0.012	24.40±2.31	0.9979

[a] Mean ± standard deviation.

For low-concentration samples, *K* was small. Higher concentration resulted in higher *K*, which can be linked to higher viscosity, as expected.

3.3 Effect of HPMC/HPS ratio on HPMC/HPS paste viscosity

Fig. 3(A) shows the effect of HPMC/HPS ratio on the viscosity of HPMC/HPS pastes. At a low HPS ratio (< 20%), the viscosity was not significantly influenced by shear rate, which could be ascribed to dispersed biopolymer chains. In contrast, the samples with a high HPS ratio showed significantly lower viscosity with increasing shear rate, a typical shear thinning behavior. At a certain shear rate, a higher HPS ratio led to higher viscosity. This corresponds to the fact that HPS is a gel with high viscosity at a low temperature (25 °C).

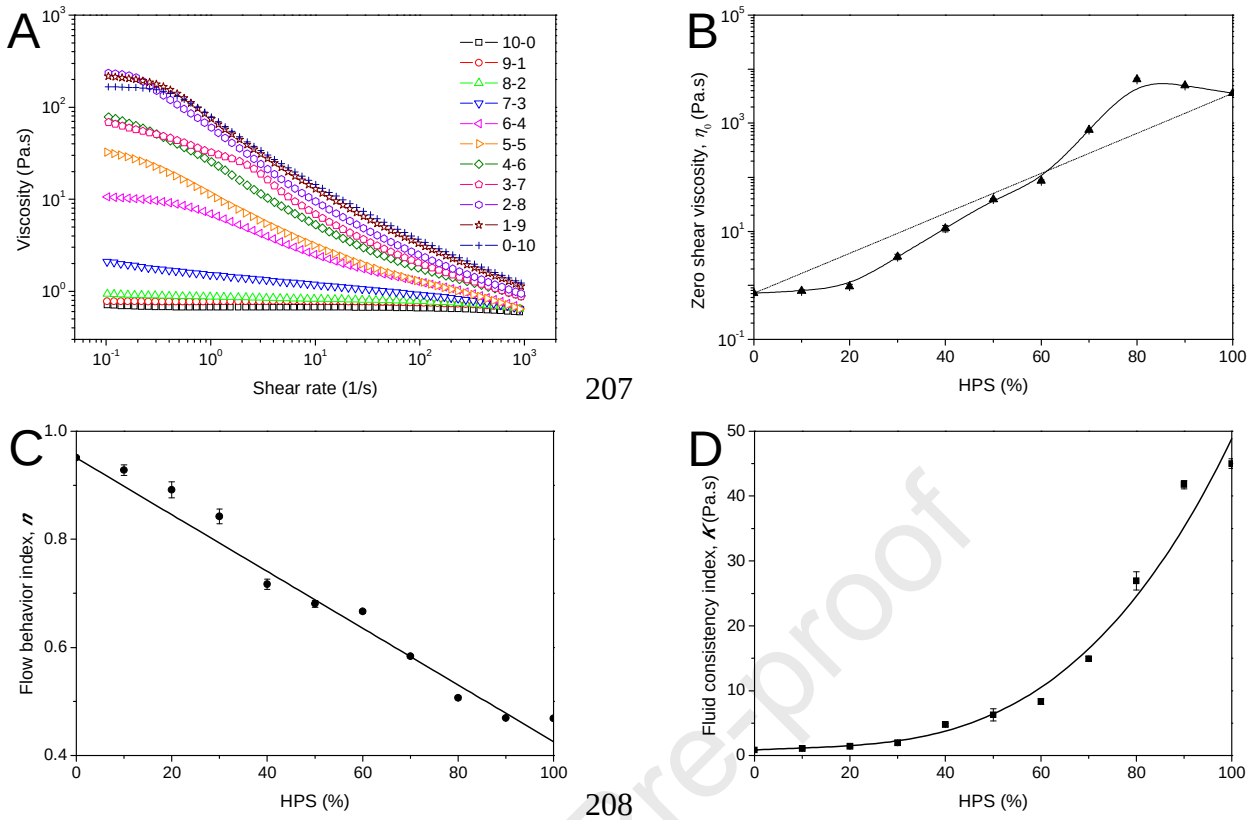

Fig. 3 A) Viscosity *vs.* shear rate curves for HPMC/HPS pastes with different HPS ratio at 25 °C; B) Zero-shear viscosity η_0, with the solid line indicating measured values and the dashed line predicted values; C) Flow behavior index *n*; and D) flow consistency index *K* for HPMC/HPS pastes with different HPS ratio. The total concentration of HPMC/HPS was 15 wt%.

Table 2 lists the *n* and *K* values for HPS/HPMC pastes with different mixing ratio. With increasing HPS ratio, *n* reduced gradually, while *K* showed a rising trend, implying that the addition of HPS made the HPMC paste more viscous and difficult to flow. This result is consistent with a previous study (Zhang, et al., 2015).

Table 2 Flow behavior index (*n*) and fluid consistency index (*K*) of HPS/HPMC solutions with different HPS/HPMC ratio at 25 °C. The total biopolymer concentration was fixed at 15 wt%.

HPMC/HPS	n	K (Pa·s^n)	R^2
10:0	0.9511±0.0023	0.84±0.01	0.9999
9:1	0.9280±0.0096	1.09±0.10	0.9998
8:2	0.8915±0.0146	1.41±0.16	0.9994
7:3	0.8423±0.0135	1.94±0.31	0.9998
6:4	0.7170±0.0094	4.76±0.20	0.9996
5:5	0.6807±0.0063	6.27±0.94	0.9993
4:6	0.6666±0.0032	8.33±0.41	0.9969
3:7	0.5835±0.0028	14.91±0.40	0.9942
2:8	0.5068±0.0037	26.93±1.39	0.9869
1:9	0.4694±0.0008	41.76±0.64	0.9897
0:10	0.4687±0.0019	45.01±0.72	0.9935

For a homogeneous system, the relationship among the rheological properties of the blend and its individual components follow a logarithmic sum rule (Utracki, 1983). For a binary system, this rule can be expressed as:

$$\log F = \phi_1 \log F_1 + \phi_2 \log F_2 \qquad (3)$$

where F, F_1, and F_2 are the rheological parameter of the mixture, component 1, and component 2, respectively; ϕ_1 and ϕ_2 are the mass fractions of component 1 and component 2, respectively, with $\phi_1 + \phi_2 = 1$.

The measured and predicted curves of η_0 as a function of HPS ratio are shown in **Fig. 3(B)**. The zero-shear viscosity increased with HPS ratio and their relationship generally follows the log-

231 additivity rule, implying good compatibility of this system. Nonetheless, the measured values deviate
232 from the mixing rule either positively or negatively, depending on HPS ratio. This suggests the
233 mixed system had a continuous-discrete type of phase structure and the change of continuous phase
234 occurred (Yao, Mukuze, Zhang, & Wang, 2013) at an HPS ratio of 60%. Regarding the negative
235 deviation at a low HPS ratio, HPMC chain existed as a continuous phase in which HPS microgel was
236 scattered. Regarding positive deviation at a high HPS ratio, HPMC became a separated phase
237 scattered in the HPS continuous phase. These results are confirmed by microscopy observation with
238 a previous study (Y. F. Wang, Zhang, et al., 2016).

239 **Fig. 3(C)** shows that *n* decreased progressively with increasing HPS ratio and the relationship
240 between *n* and HPS ratio follows the linear-additivity rule. This suggests that addition of HPS to
241 HPMC imparts stronger pseudoplastic (shear-thinning) behavior. The linear regression analysis was
242 achieved with R^2 = 0.98062, denoting good compatibility between the two biopolymers.

243 **Fig. 3(D)** shows that increasing HPS ratio resulted in higher *K*, related to the gelation behavior of
244 HPS at a low temperature. For HPMC/HPS pastes with an extreme blend ratio (HPS ratio < 20 wt%
245 or > 70 wt%), the *K* value for a blend paste is closer to that for the biopolymer with a high ratio in
246 that mixture. In this regard, the viscosity of a mixture paste is mainly determined by the continuous
247 phase. On the other hand, for HPMC/HPS pastes with an intermediate ratio (20 wt% < HPS ratio <
248 70 wt%), although HPMC with low viscosity still existed as a continuous phase, *K* rose rapidly with
249 increasing HPS ratio, indicating that HPS as the separated phase made a major contribution to the
250 viscosity of the blends. This implies that the continuous phase and the separated phase make
251 different contributions to the viscosity of a blend depending on the ratio of the two components.

3.4 Thixotropic behavior of HPMC/HPS pastes

Thixotropy describes the structural stability of a material against shear applied (Krystyjan, et al., 2016; Shakeel, Kirichek, & Chassagne, 2020; Marek Sikora, Adamczyk, & Krystyjan, 2011). Thixotropy can be linked to time and the history of shearing that results in microstructural changes (Czaikoski, da Cunha, & Menegalli, 2020; Mewis & Wagner, 2009; M. Sikora, et al., 2015). **Fig. 4** shows the results of the three-interval thixotropic behavior of HPMC/HPS pastes with different mixing ratio. All the samples were thixotropic. The viscosity at a low shear rate (1 s^{-1}, in the first and third stages) increased significantly with a higher HPS ratio.

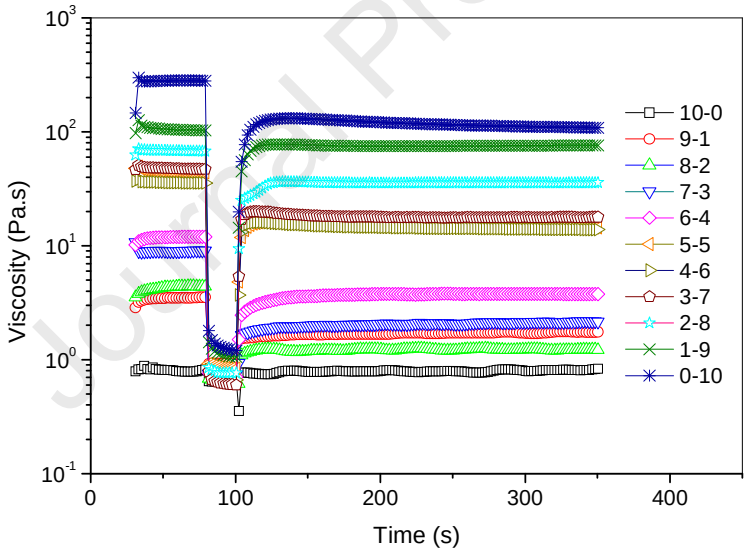

Fig. 4 Three-interval thixotropic curves for HPMC/HPS pastes with different HPMC/HPS ratio at 25 °C. The total biopolymer concentration was 15 wt%.

The structural recovery ratio (DSR) can be defined by the equation:

$$\mathrm{DSR} = \frac{\eta_t}{\eta} \times 100\% \qquad (4)$$

where η_t is the viscosity in the structural recovery stage (the third stage) at a certain time (t) and η is the final viscosity in the first stage (Mewis & Wagner, 2011; Toker, Karasu, Yilmaz, & Karaman, 2015).

With DSR < 100%, it can be assumed that the recovered paste was less resistant to shear and the material is thixotropic. In contrast, DSR > 100% indicates that the sample is anti-thixotropic. In a word, for thixotropic material, a higher DSR value means weaker thixotropic behavior (higher shear-resistance) and higher rheological stability.

The DSR data from three-interval thixotropic tests were listed in **Table 3**. The pure-HPMC solution showed a very high DSR value, close to 100%. In this regard, HPMC chains are rigid with a short relaxation time, which means the structure can recover quickly. In contrast, the pure-HPS solution presented a low DSR value. This indicates that the structural recovery of HPS is slow and can be explained by HPS chains being flexible and their long relaxation time.

Table 3 Degree of structure recovery (DSR) at certain recovery time for HPMC/HPS solutions with different HPMC/HPS ratio at 25 °C. The total biopolymer content was 15 wt%.

HPMC/HPS ratio	DSR (%)		
	10 s	60 s	250 s
10:0	91.29±1.70 [a]	93.57±0.65	98.98±0.37
9:1	63.26±2.12	66.67±2.18	71.66±1.66
8:2	39.32±0.95	42.94±0.95	45.78±1.30
7:3	20.43±0.62	22.87±0.75	24.76±0.77
6:4	24.68±0.43	30.81±0.27	31.83±0.53

5:5	37.00±1.44	36.97±1.03	34.03±0.91
4:6	44.19±0.90	41.75±0.78	38.98±0.81
3:7	59.98±1.90	53.23±1.84	50.36±1.67
2:8	57.58±0.97	58.86±0.98	59.40±0.59
1:9	67.60±0.16	72.78±0.76	72.74±1.01
0:10	38.29±0.34	45.31±0.45	38.65±0.19

[a] Mean ± standard deviation

While the DSR values for mixture pastes were lower than that for the pure-HPMC sample but higher than that for the pure-HPS sample, the change in DSR did not follow a consistent trend. For mixtures with a low HPS ratio (< 30 wt%), DSR decreased with increasing HPS ratio, indicating enhanced thixotropic behavior. In this regard, flexible HPS chains in the system counteracted the effect of rigid HPMC chains to some extent, thus decreasing the capability of the structure to recover rapidly from shear-induced deformation and prolonging the relaxation time. However, further increasing HPS content (> 30 wt%) led to an increase in DSR, suggesting weakened thixotropic behavior. In this regard, the interaction between HPMC and HPS chains might result in improvement in overall chain rigidity and thus a reduction in relaxation time.

The DSR values with different recover time are also listed in **Table 3**. HPMC/HPS pastes almost finished the structural recovery within 10 s as the DSR were very close to the final DSR (at 250 s). For some samples, the DSR values at 60 s were even high than the final DSR. Given this, these samples were more unstable as their structure could be destroyed even at very low shear rate.

3.5 Effect of temperature on the dynamic rheological properties and phase structure of HPMC/HPS pastes

As a wide range of temperature could be applied during the processing and storage of biopolymers, it is important to understand the effect of temperature on rheological properties (Park, Chung, & Yoo, 2004; Rao, 2014). Both HPMC and HPS are temperature-sensitive hydrogels and their opposite gelling behavior make it difficult to achieve a blend with high miscibility, despite these polysaccharides are chemically akin. Nevertheless, at a suitable mixing ratio and under a certain temperature, HPMC and HPS could interact with each other to the maximum extent.

3.5.1 Gelation behavior of HPMC/HPS pastes studied by dynamic viscoelasticity

The viscoelastic properties of HPMC/HPS pastes with different mixing ratio are shown in **Fig. 5 (A)**. The pure-HPMC paste showed liquid-like behavior at a low temperature as G' was below G'', while it congealed at a high temperature with G' surpassing G''. For the pure-HPS sample, the three-dimensional gel network at a low temperature solated at a high temperature, inferred from $G' < G''$. The cross point of G' and G'' was at about 49 °C for the pure-HPMC sample and 70 °C for the pure-HPS sample, confirming HPMC being a thermal gel and HPS being a cooling-gel.

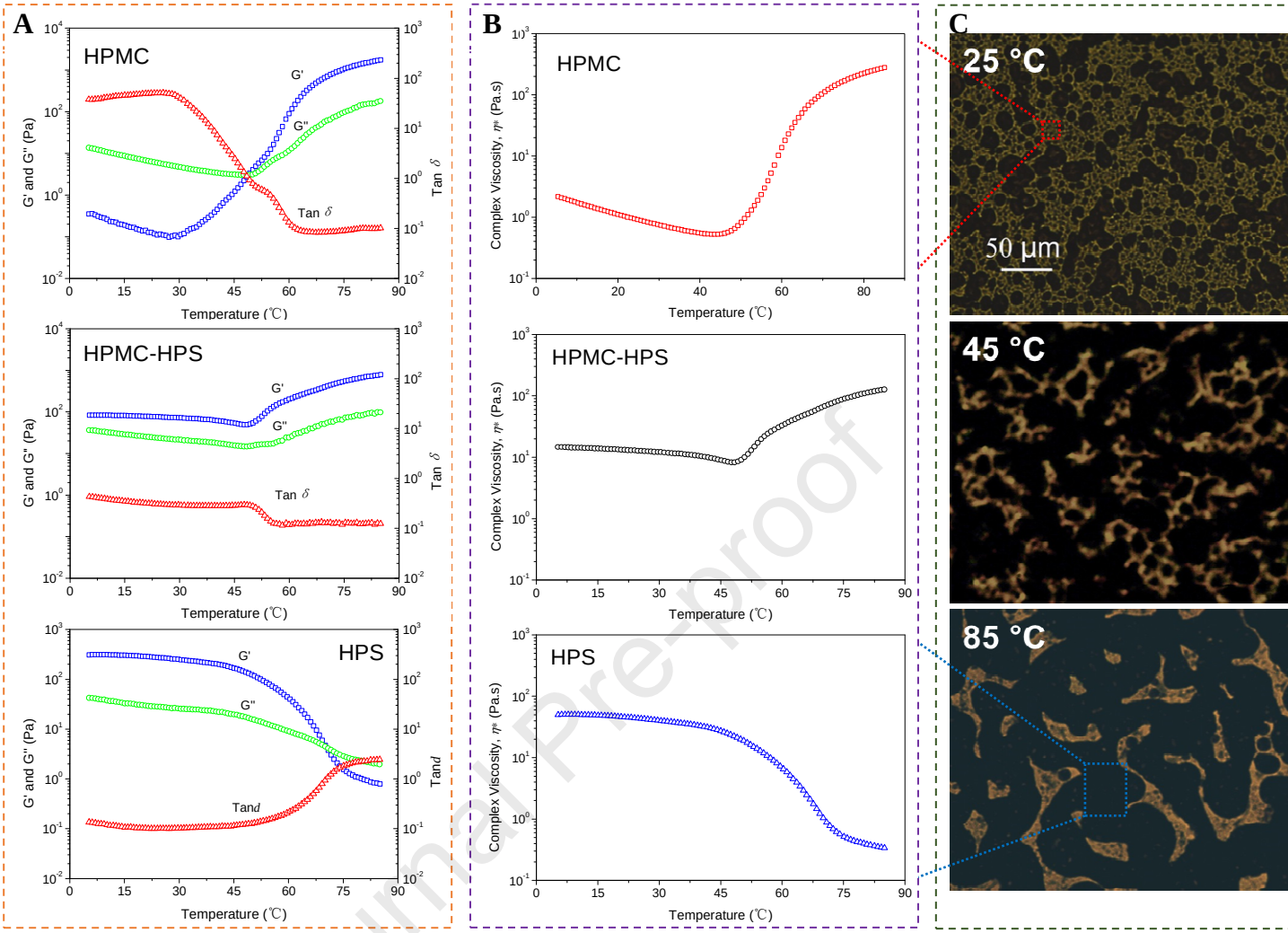

Fig. 5 A) Storage modulus (G'), loss modulus (G'') and loss tangent (tan δ) *vs.* temperature curves for the pure-HPMC paste, the 5:5 (w/w) HPMC/HPS paste, and the HPS paste, respectively, all having a total biopolymer concentration of 15 wt%; B) Complex viscosity *vs.* temperature curves for the HPMC paste, the 5:5 (w/w) HPMC/HPS paste, and the HPS paste, respectively, all having a total biopolymer concentration of 15 wt%; C) Light-microscopic images of the dyed 5:5 (w/w) HPMC/HPS paste of 3 wt% total biopolymer concentration at 25°C, 45°C, and 85 °C, respectively.

For the 5:5 (w/w) HPMC/HPS paste, the G' and G'' curves were roughly parallel to those for the pure-HPS paste at a low temperature and to those for the pure-HPMC paste at a high temperature.

Given this, HPS had a major influence on the viscoelastic properties of the mixture at a low temperature because HPS mainly contributed to the gelation at a low temperature, whereas HPMC dominated the mixture behavior at a high temperature when HPMC was responsible for gelation. The blend had intermediate moduli between those for individual HPS and HPMC. Besides, G' was always higher than G'' during the whole temperature range, indicating solid-like behavior contributed by biopolymer chain interactions. Furthermore, the 5:5 (w/w) HPMC/HPS paste showed a tan δ peak at about 45 °C, at which point a change of the continuous phase occurred.

3.5.2 Effect of temperature on the complex viscosity of HPMC/HPS pastes

For mixed systems, the viscosity of individual components is important. Normally, when two components with largely different viscosity were mixed, the component with a higher viscosity tends to form a scattered phase in the continuous phase of the lower-viscosity component.

Fig. 5(B) shows the effect of temperature on the complex viscosity (η^*) in the range of 5–85 °C of HPMC/HPS pastes. With increasing temperature, the η^* of the pure-HPS sample showed a slight decrease followed by a sharp decrease. However, the η^* of the pure-HPMC sample first experienced a slight decline and then a strong rise starting at45 °C. For the 5:5 (w/w) HPMC/HPS paste, η^* first decreased slightly and then increased moderately, a changing pattern close to that for HPS at a low temperature but similar to that for HPMC at a high temperature. This result should be ascribed to the different gelation behavior of HPS (cooling gel) and HPMC (thermal gel). The rapid change in η^* of the 5:5 (w/w) mixture at about45 °C might be due to the change in the phase distribution of HPMC/HPS.

The temperature dependence of η^* for HPMC/HPS pastes at a certain temperature can be evaluated using an Arrhenius-type equation:

$$\eta^* = \eta_i \exp\left(\alpha \frac{E}{RT}\right) \quad (5)$$

where η^* is complex viscosity, η_i is a constant describing the viscosity coefficient at a reference temperature (Pa·s) (Laity & Holland, 2017; Qing, Jinsong, Changjiang, Jianpeng, & Shouqin, 2014a), T is the absolute temperature (K), R is the gas constant (8.3144 $J \cdot mol^{-1} \cdot K^{-1}$), α is the correction coefficient (±1), and E is the activation energy ($J \cdot mol^{-1}$).

For fitting using **Eq.(5)**, the curves need to be divided into two sections before and after 45 °C according to viscosity curves shown in **Fig. 5(B)**. **Table 4** presents the values of E, α, and η_i calculated based on **Eq.(5)** for the temperature ranges of 10–45 °C and 45–85 °C ($R^2 > 0.90$). It can be seen that the η_i value for the pure-HPMC sample was very small (1.31×10^{-5} Pa·s) at a low temperature but high (1.99×10^{28} Pa·s) at a high temperature. In contrast, for the pure-HPS sample, the η_i value at a low temperature (0.56 Pa·s) was much higher than that at a high temperature (1.78×10^{-19} Pa·s). This difference in η_i between the two biopolymers could be ascribed to their different gelation behavior, namely, HPS is a cooling-gel and HPMC is a thermal-gel. For the 5:5 (w/w) blend, the η_i value was similar to that for the pure-HPS paste and much higher than that for the pure-HPMC at a low temperature, and between that for the pure-HPS sample and that for the pure-HPMC sample at a high temperature. This implies that HPS played a dominant role in the blend at a low temperature, while HPMC had a much stronger effect at a high temperature.

Table 4 Arrhenius equation parameters (correction coefficient, α; activation energy, E; constant, η_i; and determination coefficient, R^2) for the HPS paste, the 5:5 (w/w) HPS/HPMC paste, and the HPMC paste. The total biopolymer content is 15 wt%.

Sample	5–45 °C	45–85 °C

	η_i (Pa·s)	α	E (kJ·mol^{-1})	R^2	η_i (Pa·s)	α	E (kJ·mol^{-1})	R^2
HPMC	1.31×10^{-5}	+1	27.7	0.9917	1.99×10^{28}	−1	174	0.9441
HPMC-HPS	0.47	+1	8.09	0.9219	5.67×10^{12}	−1	72	0.9688
HPS	0.56	+1	10.7	0.9071	1.78×10^{-19}	+1	124	0.9744

366

367 The temperature affects biopolymer paste viscosity in different ways:

368 a) It is known that a higher temperature leads to greater chain mobility and lower viscosity.
369 Based on this effect (effect A), the viscosity is inversely proportional to temperature and α is
370 a negative value.

371 b) For a thermal gel like HPMC, increasing temperature is favorable for greater interaction
372 between hydrophobic groups and that between hydrophilic hydroxyl groups, thus enhancing
373 the three-dimensional network and increasing the viscosity. Based on this effect (effect B),
374 the viscosity is proportional to temperature and α is a positive value (Qing, Jinsong,
375 Changjiang, Jianpeng, & Shouqin, 2014b).

376 c) For a cooling gel like HPS, a higher temperature causes the breakage of intermolecular
377 hydrogen bonds and thus the three-dimensional network, leading to declined viscosity. Based
378 on this effect (effect C), the viscosity is inversely proportional to temperature and α is a
379 negative value.

380 In the low-temperature region (5–45 °C), only effect A existed for the pure-HPMC paste since it
381 was in a liquid-like state and therefore, E was high and α = +1. For the pure-HPS paste, which was a
382 solid-like gel, there were both effects A and C, while effect A was greater than effect C; thus, α = +1
383 and E was lower than that for the pure-HPMC sample. For the 5:5 (w/w) HPMC/HPS paste, both

384 effects A and C presented here, but effect C was weakened by HPMC due to its liquid-like state and
385 thus, α = +1 and E was lower than that for the pure-HPMC sample. In a word, HPS played the
386 dominant role in controlling the phase structure and rheological behavior at a low temperature.

387 In the high-temperature region (45–85 °C), both effects A and B existed for HPMC since HPMC
388 underwent gelation at a high temperature, with effect A << effect B; thus, E was very high and α =
389 −1. For HPS, there was only effect A as HPS solates at a high temperature and therefore, E was very
390 high and α = +1. For the 5:5 (w/w) mixture paste, there were both effects A and B but effect B was
391 lessened by HPS which was liquid-like; therefore, α = −1 and E was lower than that for the pure-
392 HPMC sample. These results indicate that HPMC played the leading role in controlling the structure
393 and rheological behavior of the blend at a high temperature.

394 *3.5.3* ***Effect of temperature on the phase structure of HPMC/HPS pastes***

395 **Fig. 5(C)** shows the morphologies of the 5:5 (w/w) HPMC/HPS blends at 25 °C, 45 °C, and
396 85 °C observed using an optical microscope. Two phases could be identified, the HPMC phase in
397 light and the HPS phase in dark. Under light microscopy, HPS becomes dark after being dyed with
398 iodine (Y. F. Wang, Zhang, et al., 2016). Increasing temperature resulted in an increased dark area
399 (HPS phase) but a reduced light area (HPMC phase). At 25 °C, HPMC (in light color) was shown to
400 be a continuous phase, with the scattering of small spherical HPS domains (dark). In contrast, at
401 85 °C, the HPMC phase became quite small and scattered in the HPS continuous phase.

402 There should be a certain temperature at which the viscosity of HPMC and HPS became similar,
403 thus leading to a change in the phase distribution (continuous or discrete) of the two biopolymers.
404 We observed this transition at 45 °C (**Fig. 5C)** when the typical “sea-island” morphology in the
405 blend was not shown but a pattern with two continuous phases was observable. The observation

406 agrees with the transition indicated by the tan δ peak and the rapid change in viscosity for the 5:5
407 (w/w) mixture at 45 °C.

408 **3.6 Temperature-induced structural changes of HPMC/HPS solutions**

409 Based on the comparison of HPMC/HPS blends discussed above in the context of the classic
410 rheological behavior of polymer solution and hybrid gels (Ford, 1999; Rachmawati, Woortman, &
411 Loos, 2013; Zhang, et al., 2015), we propose a schematic representation of the temperature-induced
412 conformational change of HPMC/HPS pastes, as shown in **Fig. 6**.

413 The gelation behavior of HPMC has been reported and the related mechanism has been discussed
414 (Haque & Morris, 1993; Haque, Richardson, Morris, Gidley, & Caswell, 1993; S. Q. Liu, Joshi, Lam,
415 & Tam, 2008; Viriden, Larsson, Schagerlof, & Wittgren, 2010; Y. F. Wang, et al., 2018).
416 Specifically, it is recognized that HPMC chains exist in solution as aggregated bundles. These
417 bundles are held together by the packing of the un-substituted or the sparingly soluble regions of the
418 cellulosic structure and by the hydrophobic clustering of methyl groups and hydroxyl groups in
419 regions with denser substitution. These packings and clusters are the so-called water cages and shells,
420 preventing the formation of inter-chain hydrogen bonding at a low temperature. The absorption of
421 heat can break the water cages and shells, which is kinetic of the sol-gel transition. The breakage of
422 the water cages and shells exposes methyl and hydroxyl groups to the surrounding water and causes
423 a significant increase in volume. At a higher temperature, due to both the interaction among
424 hydrophobic groups and that among hydroxyl groups, a cross-linked network is formed (**Fig. 6a**).

425 Amylose, exuded from starch granules after gelatinization, tended to coil to form hollow, left-
426 handed single helices coaxially twisting along the chains. These helices feature a hydrophobic cavity
427 inside and a hydrophilic surface outside. This compact structure of starch affords higher stability

(Lopez, de Vries, & Marrink, 2012; Rachmawati, et al., 2013; Zhou, et al., 2016). Therefore, HPS behaves as flexible random coils with stretches of helical segments in an aqueous solution at a high temperature. With reducing temperature, the hydrogen bonds between starch chains and water were broken, releasing the structured water, and inter-chain hydrogen bonding is enhanced, leading a three-dimensional gel network (**Fig. 6b**).

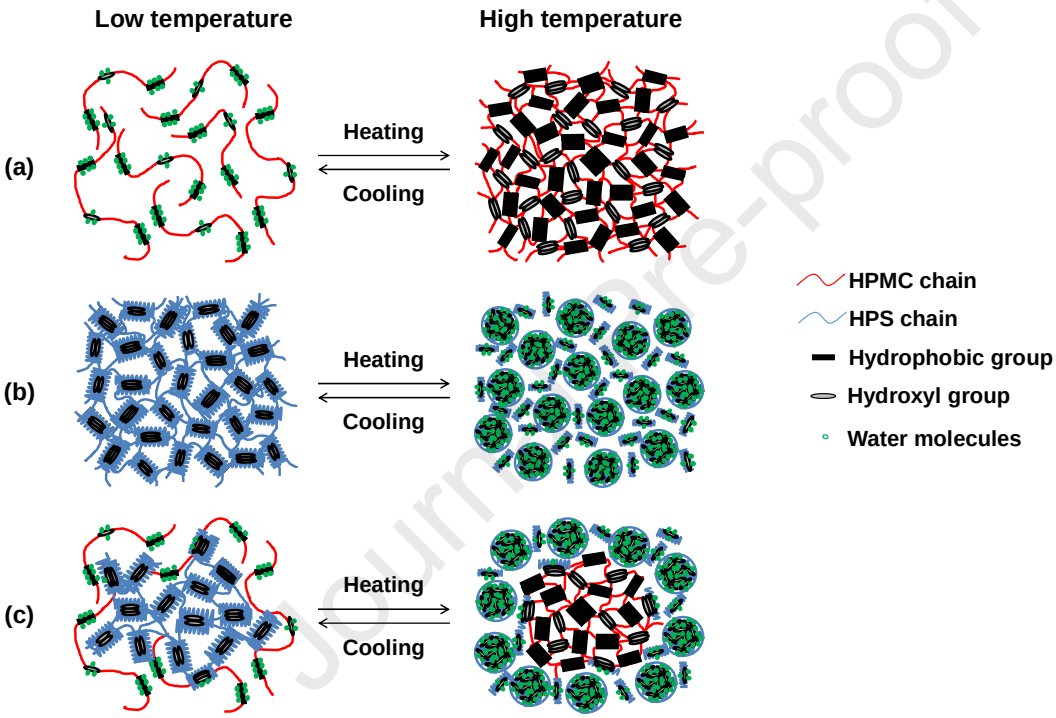

Fig.6 Schematic representation of the sol-gel transition of HPMC (a), HPS (b), and HPMC/HPS (c) pastes.

For the mixture pastes, at a low temperature, HPMC has a lower viscosity than HPS and thus HPMC forms a continuous phase encompassing discrete domains of higher-viscosity HPS gel. At the edge of the two phases, the hydroxyl groups of HPMC chains can lose the structured water and form hydrogen bonding with HPS chains. Upon heating, HPS may receive enough energy to form

hydrogen bonding with water, resulting in the gradual disintegration of the gel network. Meanwhile, the shells and water cages of HPMC chains are disrupted and even broken to expose hydroxyl groups and hydrophobic clusters. At a high temperature, HPMC forms a gel network due to the inter-chain hydrogen bonding and hydrophobic interaction and becomes a high-viscosity phase scattered in the continuous phase of HPS coils (**Fig. 6c**). Therefore, HPS at a low temperature, or HPMC at a high temperature, plays a dominant role in viscoelastic properties, gelation behavior, and phase structure for HPMC/HPS pastes.

4 Conclusion

This work reveals how the phase structure of HPMC/HPS pastes was influenced by the gelation behavior and rheological properties of individual biopolymers. And, we have established new links between rheological parameters and phase structure for such systems.

The HPMC/HPS mixture showed a typical “sea-island” phase structure. The variation in this phase conformation was significantly influenced by the viscosity of individual biopolymer, blending ratio, and temperature. With increasing HPS ratio, the continuous phase of the blend changed from HPMC to HPS at an HPS ratio of 60%. We found that this phase structure change can be well correlated to the positive or negative deviation of η_0 from the log-additivity rule.

At a low temperature, HPMC, with low viscosity, was the continuous phase, and so was HPS at a high temperature. Moreover, HPS at a low temperature, or HPMC at a high temperature, plays the dominant role in controlling the viscoelastic properties and gelation behavior. With increasing temperature, the continuous phase changed from HPS to HPMC at a critical point of 45 °C. We introduced a modified Arrhenius-type equation with correction coefficient α (±1) to explore the effect of temperature on the continuous-phase change. This phase structure change can be well

correlated to rheological indicators such as the presence of a tan δ peak, a sudden change in η^*, and the positive-negative change in α.

The results from this work led a schematic model to describe the temperature-induced conformational change of HPMC/HPS pastes, which may provide an insight into the understanding of the gelling mechanism for other temperature-sensitive multi-phasic systems.

Acknowledgements

This work was financially supported by the Doctoral Foundation of Qingdao Agricultural University (6631120081), the Program for Youth Science Innovation in Colleges and Universities in Shandong Province (2020KJF005), the Special Funds for Taishan Scholars Projects of Shandong Province (201712058), and the Research Fund of Qingdao Special Food Research Institute (66120008).

Conflicts of interest

There are no conflicts of interest to declare.

Reference

Aghjeh, M. R., Khonakdar, H. A., & Jafari, S. H. (2015). Application of mean-field theory in PP/EVA blends by focusing on dynamic mechanical properties in correlation with miscibility analysis. *Composites Part B: Engineering, 79*, 74-82.

Al-Tabakha, M. M. (2010). HPMC capsules: Current status and future prospects. *Journal of Pharmacy and Pharmaceutical ences, 13*(3), 428-442.

Allenspach, C., Timmins, P., Sharif, S., & Minko, T. (2020). Characterization of a novel hydroxypropyl methylcellulose (HPMC) direct compression grade excipient for pharmaceutical tablets. *International Journal of Pharmaceutics, 583*.

Botaro, V. R., de Freitas, R. R. M., do Carmo, K. P., & Raimundo, I. F. (2020). A simple and efficient technique to prepare aromatic polyhydroxibutirate/polybutylene adipate terephthalate blends. *Polymer Bulletin*.

Carreau, Pierre, & J. (1972). Rheological equations from molecular network theories. *Transactions of the Society of Rheology, 16*, 99-127.

Chen, R. Y., Liu, X., Han, L., Zhang, Z. H., & Li, Y. D. (2020). Morphology, thermal behavior, rheological, and mechanical properties of polypropylene/polystyrene blends based on elongation flow. *Polymers for Advanced Technologies, 31*(11), 2722-2732.

Chen, X., Cui, F. H., Zi, H., Zhou, Y. C., Liu, H. S., & Xiao, J. (2019). Development and characterization of a hydroxypropyl starch/zein bilayer edible film. *International Journal of Biological Macromolecules, 141*, 1175-1182.

Colby, R. H. (2010). Structure and linear viscoelasticity of flexible polymer solutions: comparison of polyelectrolyte and neutral polymer solutions. *Rheologica Acta, 49*(5), 425-442.

Cuq, B., Gontard, N., & Guilbert, S. (1998). Proteins as agricultural polymers for packaging production. *Cereal Chemistry, 75*(1), 1-9.

Czaikoski, A., da Cunha, R. L., & Menegalli, F. C. (2020). Rheological behavior of cellulose nanofibers from cassava peel obtained by combination of chemical and physical processes. *Carbohydrate Polymers, 248*.

Ford, J. L. (1999). Thermal analysis of hydroxypropylmethylcellulose and methylcellulose: powders, gels and matrix tablets. *International Journal of Pharmaceutics, 179*(2), 209-228.

Ghadermazi, R., Hamdipour, S., Sadeghi, K., Ghadermazi, R., & Asl, A. K. (2019). Effect of various additives on the properties of the films and coatings derived from hydroxypropyl methylcellulose-A review. *Food Science & Nutrition, 7*(11), 3363-3377.

Haque, A., & Morris, E. R. (1993). Thermogelation of methylcellulose .1. Molecular-structures and processes. *Carbohydrate Polymers, 22*(3), 161-173.

Haque, A., Richardson, R. K., Morris, E. R., Gidley, M. J., & Caswell, D. C. (1993). Thermogelation of methylcellulose .2. Effect of hydroxypropyl substituents. *Carbohydrate Polymers, 22*(3), 175-186.

Hay, W. T., Fanta, G. F., Peterson, S. C., Thomas, A. J., Utt, K. D., Walsh, K. A., Boddu, V. M., & Selling, G. W. (2018). Improved hydroxypropyl methylcellulose (HPMC) films through incorporation of amylose-sodium palmitate inclusion complexes. *Carbohydrate Polymers, 188*, 76-84.

Ilyin, S. O., Makarova, V. V., Polyakova, M. Y., & Kulichikhin, V. G. (2020). Phase behavior and rheology of miscible and immiscible blends of linear and hyperbranched siloxane macromolecules. *Materials Today Communications, 22*.

Jéssica Bassi da Silva, Michael Thomas Cook, & Bruschi, M. L. (2020). Thermoresponsive systems composed of poloxamer 407 and HPMC or NaCMC: mechanical, rheological and sol-gel transition analysis. *Carbohydrate Polymers, 240*.

Krystyjan, M., Sikora, M., Adamczyk, G., Dobosz, A., Tomasik, P., Berski, W., Lukasiewicz, M., & Izak, P. (2016). Thixotropic properties of waxy potato starch depending on the degree of the granules pasting. *Carbohydr Polym, 141*, 126-134.

Laity, P. R., & Holland, C. (2017). Thermo-rheological behaviour of native silk feedstocks. *European Polymer Journal, 87*, 519-534.

Liu, J., Lai, R., Wang, X. L., Wang, H. Y., & Liu, Y. W. (2020). Preparation and characterization of composites of hydroxypropyl tapioca starch and zein. *Starch-Starke, 72*(1-2).

Liu, S. Q., Joshi, S. C., Lam, Y. C., & Tam, K. C. (2008). Thermoreversible gelation of hydroxypropylmethylcellulose in simulated body fluids. *Carbohydrate Polymers, 72*(1), 133-143.

Lopez, C. A., de Vries, A. H., & Marrink, S. J. (2012). Amylose folding under the influence of lipids. *Carbohydrate Research, 364*, 1-7.

Mewis, J., & Wagner, N. J. (2009). Thixotropy. *Advances in Colloid and Interface Science, 147-48*, 214-227.

Mewis, J., & Wagner, N. J. (2011). Colloidal Suspension Rheology: Thixotropy. *10.1017/CBO9780511977978*(7), 228-251.

Morris, E. R., Cutler, A. N., Ross-Murphy, S. B., Rees, D. A., & Price, J. (1981). Concentration and shear rate dependence of viscosity in random coil polysaccharide solutions. *Carbohydrate Polymers, 1*(1), 5-21.

Muhammad-Javeed, A., & Mohammed, A. (2018). Study of the barrier and mechanical properties of packaging edible films fabricated with hydroxypropyl methylcellulose (HPMC) combined with electro-activated whey. *Journal of Packaging Technology and Research*.

Pakravan, M., Heuzey, M. C., & Ajji, A. (2011). A fundamental study of chitosan/PEO electrospinning. *Polymer, 52*(21), 4813-4824.

Park, S., Chung, M. G., & Yoo, B. (2004). Effect of octenylsuccinylation on rheological properties of corn starch pastes. *Starch-Starke, 56*(9), 399-406.

Peressini, D., Bravin, B., Lapasin, R., Rizzotti, C., & Sensidoni, A. (2003). Starch-methylcellulose based edible films: rheological properties of film-forming dispersions. *Journal of Food Engineering, 59*(1), 25-32.

Polamaplly, P., Cheng, Y. L., Shi, X. L., Manikandan, K., Zhang, X., Kremer, G. E., & Qin, H. T. (2019). 3D printing and characterization of hydroxypropyl methylcellulose and methylcellulose for biodegradable support structures. *Polymer, 173*, 119-126.

Qin, Y., Wang, W. T., Zhang, H., Dai, Y. Y., Hou, H. X., & Dong, H. Z. (2019). Effects of citric acid on structures and properties of thermoplastic hydroxypropyl amylomaize starch films. *Materials, 12*(9).

Qing, L., Jinsong, Z., Changjiang, X., Jianpeng, D., & Shouqin, Z. (2014a). Influence of temperature, pH, and ionic strength on the rheological properties of oviductus ranae hydrogels. *African Journal of Biotechnology, 13*(24), 2435-2444.

Qing, L., Jinsong, Z., Changjiang, X., Jianpeng, D., & Shouqin, Z. (2014b). Influence of temperature, pH, and ionic strength on the rheological properties of oviductus ranae hydrogels. *African Journal of Biotechnology, 13*(24).

Rachmawati, R., Woortman, A. J., & Loos, K. (2013). Tunable properties of inclusion complexes between amylose and polytetrahydrofuran. *Macromolecular Bioscience, 13*(6), 767-776.

Rao, M. A. (2014). Flow and functional models for rheological properties of fluid foods. In T. Dura (Ed.), *Rheology of Fluid, Semisolid, and Solid Foods* (pp. 27-61). US: Springer.

Shakeel, A., Kirichek, A., & Chassagne, C. (2020). Rheological analysis of mud from Port of Hamburg, Germany. *Journal of Soils and Sediments, 20*(6), 2553-2562.

Siepmann, J., & Peppas, N. A. (2012). Modeling of drug release from delivery systems based on hydroxypropyl methylcellulose (HPMC). *Advanced Drug Delivery Reviews, 64*, 163-174.

Sikora, M., Adamczyk, G., & Krystyjan, M. (2011). Thixotropy as a measure of liquid food producs *Zywnosc-Nauka Technologia Jakosc, 18*(1), 5-14.

Sikora, M., Adamczyk, G., Krystyjan, M., Dobosz, A., Tomasik, P., Berski, W., Lukasiewicz, M., & Izak, P. (2015). Thixotropic properties of normal potato starch depending on the degree of the granules pasting. *Carbohydr Polym, 121*, 254-264.

Suhag, R., Kumar, N., Petkoska, A. T., & Upadhyay, A. (2020). Film formation and deposition methods of edible coating on food products: A review. *Food Research International, 136*.

Tajuddin, S., Xie, F., Nicholson, T. M., Liu, P., & Halley, P. J. (2011). Rheological properties of thermoplastic starch studied by multipass rheometer. *Carbohydrate Polymers, 83*(2), 914-919.

Tan, X., Li, X., Chen, L., & Xie, F. (2016). Solubility of starch and microcrystalline cellulose in 1-ethyl-3-methylimidazolium acetate ionic liquid and solution rheological properties. *Physical Chemistry Chemical Physics*, 27584-27593.

Tanaka, Y., Sako, T., Hiraoka, T., Yamaguchi, M., & Yamaguchi, M. (2020). Effect of morphology on shear viscosity for binary blends of polycarbonate and polystyrene. *Journal of Applied Polymer Science, 137*(46).

Toker, O. S., Karasu, S., Yilmaz, M. T., & Karaman, S. (2015). Three interval thixotropy test (3ITT) in food applications: A novel technique to determine structural regeneration of mayonnaise under different shear conditions. *Food Research International, 70*(apr.), 125-133.

Utracki, L. A. (1983). Melt flow of polymer blends. *Polymer Engineering and ence, 23*(11), 602-609.

Viriden, A., Larsson, A., Schagerlof, H., & Wittgren, B. (2010). Model drug release from matrix tablets composed of HPMC with different substituent heterogeneity. *International Journal of Pharmaceutics, 401*(1-2), 60-67.

Wang, Q., Yang, Y. H., Chen, X., & Shao, Z. Z. (2012). Investigation of rheological properties and conformation of silk fibroin in the solution of amimcl. *Biomacromolecules, 13*(6), 1875-1881.

Wang, W. W., Sun, Z. H., & Shi, Y. C. (2019). An improved method to determine the hydroxypropyl content in modified starches by H-1 NMR. *Food Chemistry, 295*, 556-562.

Wang, Y. F., Yu, L., Xie, F. W., Li, S., Sun, Q. J., Liu, H. S., & Chen, L. (2018). On the investigation of thermal/cooling-gel biphasic systems based on hydroxypropyl methylcellulose and hydroxypropyl starch. *Industrial Crops and Products, 124*, 418-428.

Wang, Y. F., Yu, L., Xie, F. W., Zhang, L., Liao, L., Liu, H. S., & Chen, L. (2016). Morphology and properties of thermal/cooling-gel bi-phasic systems based on hydroxypropyl methylcellulose and hydroxypropyl starch. *Composites Part B-Engineering, 101*, 46-52.

Wang, Y. F., Zhang, L., Liu, H. S., Yu, L., Simon, G. P., Zhang, N. Z., & Chen, L. (2016). Relationship between morphologies and mechanical properties of hydroxypropyl methylcellulose/hydroxypropyl starch blends. *Carbohydrate Polymers, 153*, 329-335.

Wongphan, P., & Harnkarnsujarit, N. (2020). Characterization of starch, agar and maltodextrin blends for controlled dissolution of edible films. *International Journal of Biological Macromolecules, 156*, 80-93.

Xiao, Q., Tong, Q. Y., & Lim, L. T. (2012). Pullulan-sodium alginate based edible films: Rheological properties of film forming solutions. *Carbohydrate Polymers, 87*(2), 1689-1695.

Xiao, Q., Tong, Q. Y., Zhou, Y. J., & Deng, F. M. (2015). Rheological properties of pullulan-sodium alginate based solutions during film formation. *Carbohydrate Polymers, 130*, 49-56.

Xu, Y. P., Wang, T., & Shi, X. (2020). Enhanced dielectric and capacitive performance in polypropylene/poly (vinylidene fluoride) binary blends compatibilized with polydopamine. *Materials & Design, 195*.

Yao, Y., Mukuze, K. S., Zhang, Y., & Wang, H. (2013). Rheological behavior of cellulose/silk fibroin blend solutions with ionic liquid as solvent. *Cellulose, 21*(1), 675-684.

Zhang, L., Wang, Y. F., Liu, H. S., Zhang, N. Z., Liu, X. X., Chen, L., & Yu, L. (2013). Decelopment of capsules from natural plan polymers. *Acta Polymerica Sinica*(1), 1-10.

Zhang, L., Wang, Y. F., Yu, L., Liu, H. S., Simon, G., Zhang, N. Z., & Chen, L. (2015). Rheological and gel properties of hydroxypropyl methylcellulose/hydroxypropyl starch blends. *Colloid and Polymer Science, 293*(1), 229-237.

618 Zhong, M. M., Xie, F. Y., Zhang, S., Sun, Y. F., Qi, B. K., & Li, Y. (2020). Preparation and digestive
619 characteristics of a novel soybean lipophilic protein-hydroxypropyl methylcellulose-calcium chloride
620 thermosensitive emulsion gel. *Food Hydrocolloids*, *106*.
621 Zhou, Y., Li, X., Lv, Y., Shi, Y., Zeng, Y., Li, D., & Mu, C. (2016). Effect of oxidation level on the inclusion
622 capacity and solution stability of oxidized amylose in aqueous solution. *Carbohydrate Polymers*, *138*,
623 41-48.

624

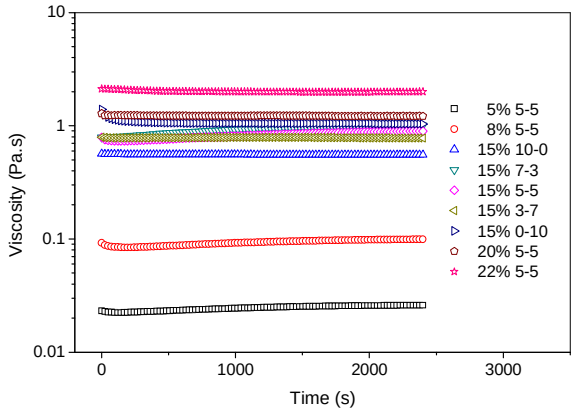

Fig. 1 Viscosity as a function of time for HPMC/HPS pastes. The shear rate was fixed at 800 s^{-1}.

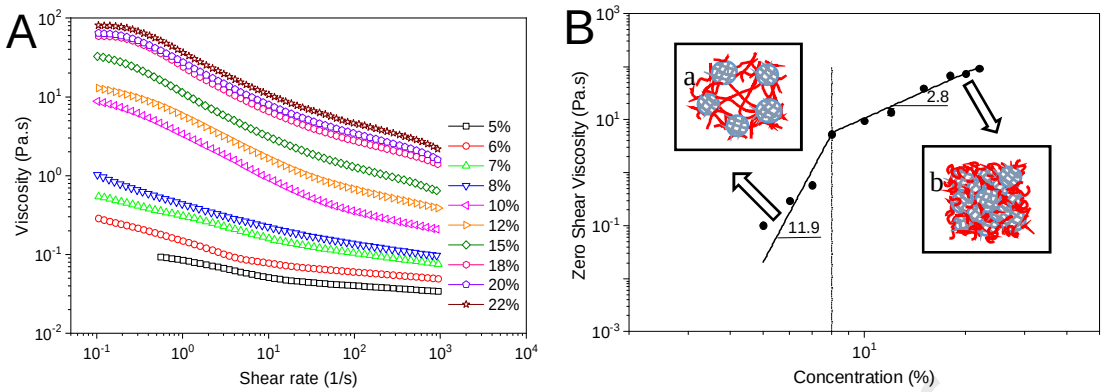

Fig. 2 A) Flow curves for 50:50 (w/w) HPMC/HPS pastes of different total biopolymer concentration at 25 °C; B) Zero-shear viscosity as a function of total biopolymer concentration, with the molecular conformation of HPMC/HPS schematically shown (the HPMC/HPS ratio was 50:50 (w/w), red lines represent HPMC chains and grey lines HPS).

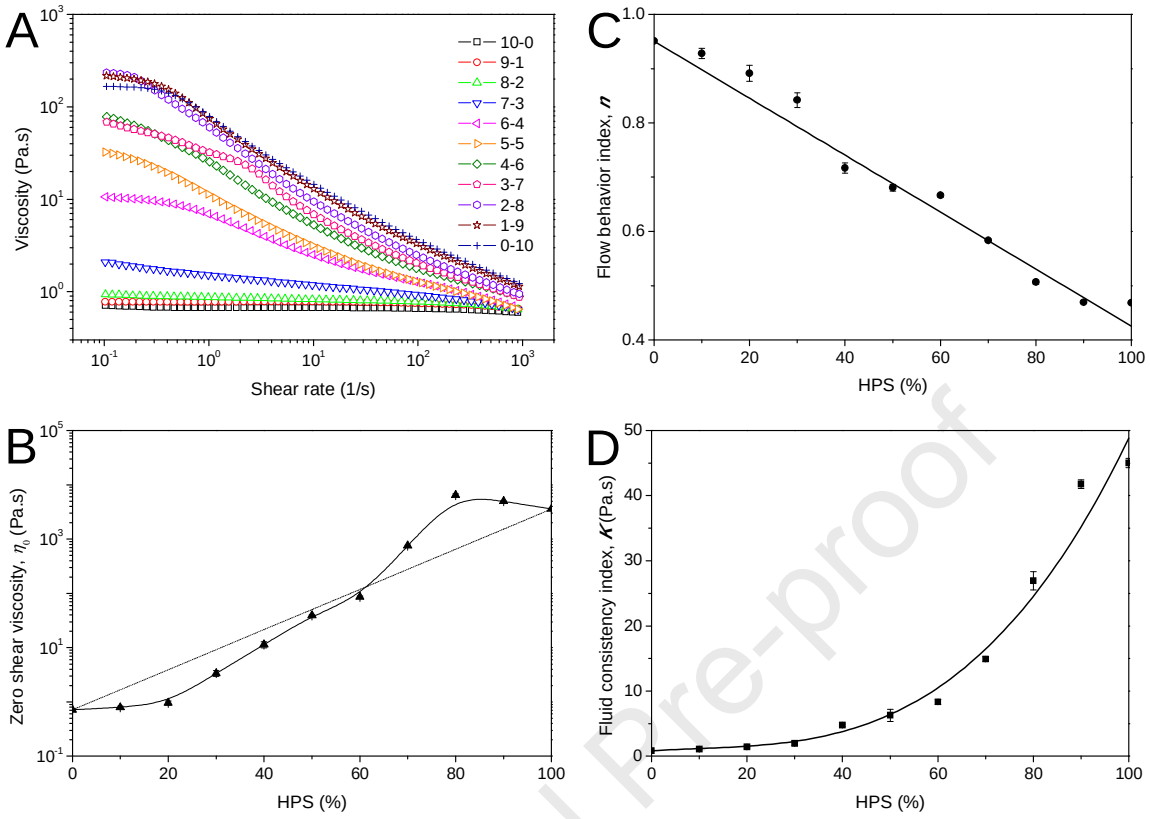

Fig.3 A) Viscosity *vs.* shear rate curves for HPMC/HPS pastes with different HPS ratio at 25 °C; B) Zero-shear viscosity η_0, with the solid line indicating measured values and the dashed line predicted values; C) Flow behavior index *n*; and D) flow consistency index *K* for HPMC/HPS pastes with different HPS ratio. The total concentration of HPMC/HPS was 15 wt%.

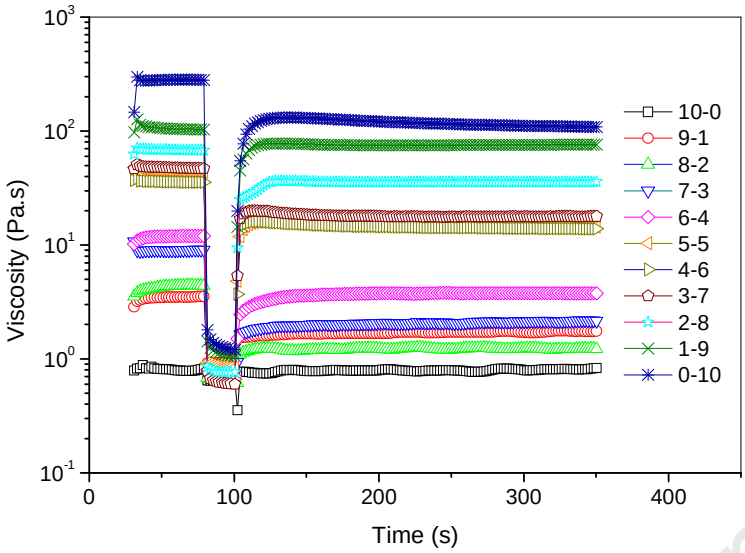

Fig. 4 Three-interval thixotropic curves for HPMC/HPS pastes with different HPMC/HPS ratio at 25 °C. The total biopolymer concentration was 15 wt%.

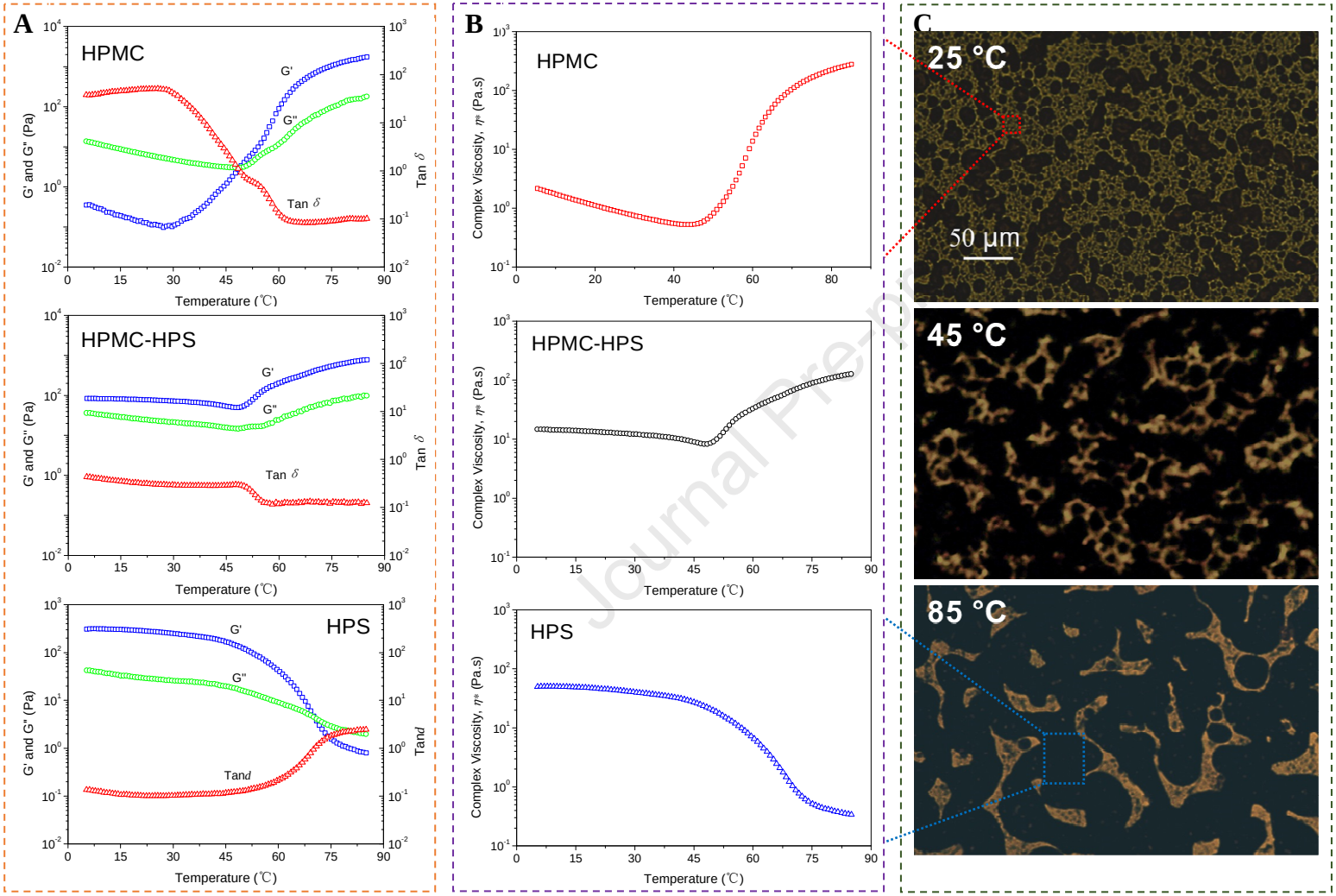

Fig.5. A) Storage modulus (*G′*), loss modulus (*G″*) and loss tangent (tan *δ*) *vs.* temperature curves for the pure-HPMC paste, the 5:5 (w/w) HPMC/HPS paste, and the HPS paste, respectively, all having a total biopolymer concentration of 15 wt%; B) Complex viscosity *vs.* temperature curves for the HPMC paste, the 5:5 (w/w) HPMC/HPS paste, and the HPS paste, respectively, all having a total biopolymer concentration of 15 wt%; C) Light-microscopic images of the dyed 5:5 (w/w) HPMC/HPS paste of 3 wt% total biopolymer concentration at 25 °C, 45 °C, and 85 °C, respectively.

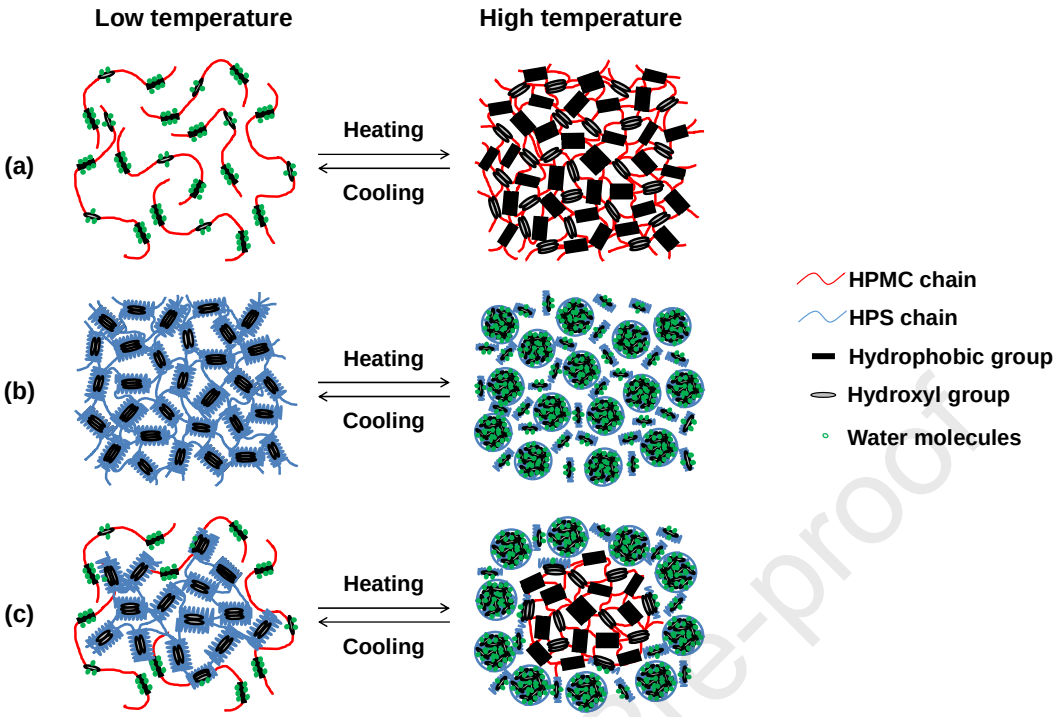

Fig. 6 Schematic representation of the sol-gel transition of HPMC (a), HPS (b), and HPMC/HPS (c) pastes.

Highlights:

- ✓ Hydroxypropyl methylcellulose (HPMC) and hydroxypropyl starch (HPS) mixture studied
- ✓ Strong rheological and gelation effects on the phase structure of HPMC/HPS shown
- ✓ HPMC/HPS blend ratio and temperature controls continuous/discrete phase change
- ✓ Phase structure correlated to zero-shear viscosity and Arrhenius coefficient α
- ✓ A schematic model to describe the temperature-induced conformational change

– Declaration of Interest –

Hydroxypropyl methylcellulose and hydroxypropyl starch: Rheological and gelation effects on the phase structure of their mixed hydrocolloid system

Yanfei Wang[1,2,3], Long Yu[3], Qingjie Sun[1,2], Fengwei Xie[4]

[1]*College of Food Science and Engineering, Qingdao Agricultural University, Qingdao, Shandong 266109, China*

[2]*Qingdao Special Food Research Institute, Qingdao, Shandong 266109, China*

[3]*College of Food Science and Engineering, South China University of Technology, Guangzhou, Guangdong 510640, China*

[4]*International Institute for Nanocomposites Manufacturing (IINM), WMG, University of Warwick, Coventry CV4 7AL, United Kingdom*

The authors declare that there is no conflict of interest regarding the publication of this article.